AFRL-VA-WP-TM-2003-3085

A COOPERATIVE RANGE DELAY DECEPTION-BASED APPROACH TO MULTIPLE RADAR PHANTOM TRACKS

Scott Waun

Control Theory Optimization Branch (AFRL/VACA)
Control Sciences Division
Air Vehicles Directorate
Air Force Research Laboratory, Air Force Materiel Command
Wright-Patterson Air Force Base, OH 45433-7542

SEPTEMBER 2003

Final Report for 01 June 2003 – 01 September 2003

Approved for public release; distribution is unlimited.

STINFO FINAL REPORT

AIR VEHICLES DIRECTORATE
AIR FORCE RESEARCH LABORATORY
AIR FORCE MATERIEL COMMAND
WRIGHT-PATTERSON AIR FORCE BASE, OH 45433-7542

20040112 171

REPORT DOCUMENTATION PAGE

Form Approved
OMB No. 0704-0188

The public reporting burden for this collection of information is estimated to average 1 hour per response, including the time for reviewing instructions, searching existing data sources, searching existing data sources, gathering and maintaining the data needed, and completing and reviewing the collection of information. Send comments regarding this burden estimate or any other aspect of this collection of information, including suggestions for reducing this burden, to Department of Defense, Washington Headquarters Services, Directorate for Information Operations and Reports (0704-0188), 1215 Jefferson Davis Highway, Suite 1204, Arlington, VA 22202-4302. Respondents should be aware that notwithstanding any other provision of law, no person shall be subject to any penalty for failing to comply with a collection of information if it does not display a currently valid OMB control number. **PLEASE DO NOT RETURN YOUR FORM TO THE ABOVE ADDRESS.**

1. REPORT DATE *(DD-MM-YY)*	2. REPORT TYPE	3. DATES COVERED *(From - To)*
September 2003	Final	06/01/2003 – 09/01/2003

4. TITLE AND SUBTITLE

A COOPERATIVE RANGE DELAY DECEPTION-BASED APPROACH TO MULTIPLE RADAR PHANTOM TRACKS

5a. CONTRACT NUMBER
IN-HOUSE

5b. GRANT NUMBER

5c. PROGRAM ELEMENT NUMBER
N/A

6. AUTHOR(S)

Scott Waun

5d. PROJECT NUMBER
N/A

5e. TASK NUMBER
N/A

5f. WORK UNIT NUMBER
N/A

7. PERFORMING ORGANIZATION NAME(S) AND ADDRESS(ES)

Control Theory Optimization Branch (AFRL/VACA)
Control Sciences Division
Air Vehicles Directorate
Air Force Research Laboratory, Air Force Materiel Command
Wright-Patterson Air Force Base, OH 45433-7542

8. PERFORMING ORGANIZATION REPORT NUMBER

AFRL-VA-WP-TM-2003-3085

9. SPONSORING/MONITORING AGENCY NAME(S) AND ADDRESS(ES)

Air Vehicles Directorate
Air Force Research Laboratory
Air Force Materiel Command
Wright-Patterson Air Force Base, OH 45433-7542

10. SPONSORING/MONITORING AGENCY ACRONYM(S)

AFRL/VACA

11. SPONSORING/MONITORING AGENCY REPORT NUMBER(S)

AFRL-VA-WP-TM-2003-3085

12. DISTRIBUTION/AVAILABILITY STATEMENT
Approved for public release; distribution is unlimited.

13. SUPPLEMENTARY NOTES

14. ABSTRACT *(Maximum 200 Words)*
A radar deception scenario that employs a cooperative multi-agent team is considered as an example of a more general distributed nonformation cooperative control problem. The team uses range-delay based deception techniques to cooperatively project a phantom track to a system of radars. The problem is characterized and the geometry analyzed using different sets of constraints. A distributed cooperative control problem is formally stated and a solution is presented. Finally, the solution is extended and other aspects of the problem are considered.

15. SUBJECT TERMS
ELECTRONIC DECEPTION RADAR SYSTEM, ARBITRARY RADAR AND AIRCRAFT

16. SECURITY CLASSIFICATION OF:			17. LIMITATION OF ABSTRACT:	18. NUMBER OF PAGES	19a. NAME OF RESPONSIBLE PERSON (Monitor)
a. REPORT Unclassified	**b. ABSTRACT** Unclassified	**c. THIS PAGE** Unclassified	SAR	18	Reid A. Larson **19b. TELEPHONE NUMBER** *(Include Area Code)* (937) 255-6301

Standard Form 298 (Rev. 8-98)
Prescribed by ANSI Std. Z39-18

A Cooperative Range Delay Deception-Based Approach to Multiple Radar Phantom Tracks

Scott Waun

Electrical Engineering, Ohio State University, Columbus, Ohio 43210
Air Force Research Laboratory, Air Vehicles Directorate, WPAFB, OH 45433

September 23, 2003

Abstract

A radar deception scenario that employs a cooperative multi-agent team is considered as an example of a more general distributed non-formation cooperative control problem. The team uses range-delay based deception techniques to cooperatively project a phantom track to a system of radars. The problem is characterized and the geometry analyzed using different sets of constraints. A distributed cooperative control problem is formally stated and a solution is presented. Finally, the solution is extended and other aspects of the problem are considered.

1 Introduction

Much of the study of cooperative control has focused on the area of formation control. This is due, in part, to the fact that many of these problems reduce to single-agent control problems. Because of the tightly coupled dynamics of the systems, a hierarchical approach can be taken to decompose the problems into simpler ones. Many cooperative control problems lie outside this area, however. Problems such as coordinated rendezvous or cooperative task assignment fall outside the scope, but are of greater practical importance. Another example of a non-formation cooperative control problem that warrants study is that of cooperative radar deception.
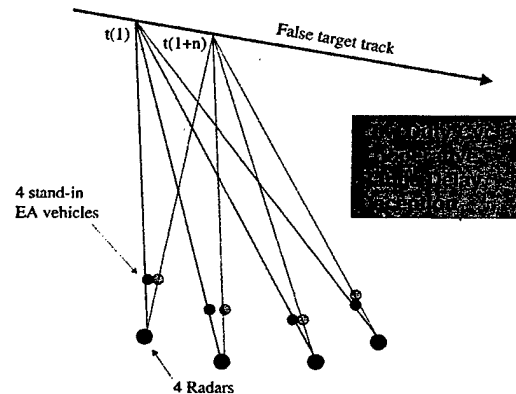

Figure 1.1: Radar Deception Scenario

It is assumed, for now, that our chosen radar employs low-duty cycle, low Pulse Repetition Frequency (PRF) radar, in a tracking mode. In addition, it is assumed that pulse encryption is employed, preventing the cross-contamination of radar signals. This will be referred to as "pulse agility". The deception strategy considered here is to employ a network of Electronic Combat Air Vehicles (ECAVs) that will intercept radar pulses, delay and retransmit them. By inserting this range delay, an individual ECAV can project a collinear "phantom" point in space. If multiple vehicles coordinate their positions and delays, the phantom points will converge and the radar network will be deceived. Through coordinated trajectory planning, the vehicles can make this phantom point move in a phantom trajectory. In addition, it may be possible to generate more than one phantom track by manipulating secondary effects of the radars.

Two principle physical constraints are speed and heading of the ECAVs and phantom track. The speed constraint can be imposed as either a minimum stall speed or as a constant speed. The heading can either be restricted such that its antenna always faces the radar, or as a minimum turn radius constraint. Also, because of the pulse agility, it is assumed that the ECAV must stay between the phantom point and the radar station. That is, the phantom track must be beyond the ECAV in range and thus the pulse delay must be a positive number.

The problem can be posed in one of two ways. In one scenario, the ECAVs fly specified trajectories, with the possible phantom track(s) unknown. This will be referred to as the direct problem. Alternatively, the phantom track can be specified and the requisite ECAV trajectories chosen. This will be called the inverse problem. The direct problem is not as interesting, due to the lack of freedom it provides. Given a set of arbitrary ECAV trajectories, there is little chance that a phantom track can converge.

There are several approaches to the solution of this problem. In the inverse problem, solutions can take the form of continuous trajectories or as discreet waypoints. The ECAV trajectories can either be decided *a priori* (offline), or can be determined iteratively based on the current state of the ECAVs (online). In the offline case, the vehicle trajectories are determined by solving an optimization problem ahead of time. If the system is highly time-synchronized, the offline case can be considered an open-loop problem. The online control problem can be centralized or decentralized, depending on the performance requirements.

The objective of this paper is to analyze the feasibility of the inverse radar deception scenario, as described. First the single ECAV, single phantom problem is considered to analyze the problem geometry. Next, the results are extended to the multiple ECAV, single phantom case. Finally, the multiple phantoms, multiple ECAV case is considered. An effort has been made to abstract specific radar capabilities from the analysis. This is not wholly possible in the multiple phantoms case, however. Other radar-specific considerations are discussed and conclusions are drawn on the feasibility of this scenario.

2 Single ECAV, Single Phantom

The geometric analysis in this paper is two-dimensional because the ECAV ranges are so great that elevation changes are considered negligible. It is assumed that the radars measure only azimuth and range.

In this section, we will consider the case of a single ECAV trying to project a single phantom to a single radar station. This analysis only serves to uncover the geometric relationships inherent to the problem. When there is only one radar station, radar network substantiation is not an issue. At this time, it is assumed that the phantom track is predefined. Because there is only one ECAV in this scenario, track negotiation becomes trivial. This analysis also applies to the single ECAV, multiple phantoms case. The ECAV can generate any number of phantom tracks simply by inserting multiple returns with varying delay.

The scenario can be analyzed using any combination of constraints. Rather than exhaustively checking the sensitivity to each constraint, a few representative cases will be selected. First, the minimum velocity/unconstrained angle case will be considered to generate a discreet formulation of the problem in Cartesian coordinates. Next, the constant velocity/constrained angle case will be considered.

2.1 Minimum Velocity, Unconstrained Angle

Given:

$V_p(t)$: Linear velocity of phantom trajectory

$\psi_p(t)$: Heading of phantom trajectory

x_r, y_r : Position of radar station

$x_u(0), y_u(0)$: Initial position of ECAV

Find:

$V_u(t)$: Linear velocity of ECAV

$\psi_u(t)$: Heading of ECAV

2

Figure 2.1: Cartesian Coordinate System

Solution:

$$\hat{x} = x - x_r$$

$$\hat{y} = y - y_r$$

$$\hat{x}_p(t) = \int_0^t V_p(T)\sin\psi_p(T)dT$$

$$\hat{y}_p(t) = \int_0^t V_p(T)\cos\psi_p(T)dT$$

$$\hat{r}_p(t) = \sqrt{\hat{x}_p^2 + \hat{y}_p^2}$$

$$\hat{r}_u(t) = \alpha(t)\hat{r}_p(t)$$

$$\psi_r(t) = \operatorname{atan}(\hat{x}_p(t)/\hat{y}_p(t))$$

$$\hat{x}_u(t) = \hat{r}_u(t)\sin\psi_r(t)$$
$$= \alpha(t)\hat{x}_p(t)$$
$$\hat{y}_u(t) = \hat{r}_u(t)\cos\psi_r(t)$$
$$= \alpha(t)\hat{y}_p(t)$$

$$\hat{x}_u(t) = \int_0^t V_u(T)\sin\psi_u(T)dT$$

$$\hat{y}_u(t) = \int_0^t V_u(T)\cos\psi_u(T)dT$$

$$\alpha(t) = \frac{\int_0^t V_u(T)\sin\psi_u(T)dT}{\hat{x}_p(t)} = \frac{\int_0^t V_u(T)\cos\psi_u(T)dT}{\hat{y}_p(t)}$$

$$\hat{y}_p^{i+1}(\hat{x}_u^i + V_u^i\sin\psi_u^i\Delta t) = \hat{x}_p^{i+1}(\hat{y}_u^i + V_u^i\cos\psi_u^i\Delta t)$$

$$V_u^i(\psi_u^i) = \frac{\hat{x}_p^{i+1}\hat{y}_u^i - \hat{y}_p^{i+1}\hat{x}_u^i}{(\hat{y}_p^{i+1}\sin\psi_u^i - \hat{x}_p^{i+1}\cos\psi_u^i)\Delta t}$$

Constraints:

$$0 < \alpha^i < 1 \Rightarrow \operatorname{atan}(\frac{\hat{x}_p^{i+1} - \hat{x}_u^i}{\hat{y}_p^{i+1} - \hat{y}_u^i}) < \psi_u^i < \psi_r^i + \pi$$

$$V_u^i > V_{\min} \Rightarrow \psi_u^i(V_{\min})^- < \psi_u^i < \psi_u^i(V_{\min})^+$$

$$\psi_u^i(V_u^i) = -j\ln\left(\frac{c^i \pm \sqrt{(c^i)^2 - (\hat{y}_p^{i+1})^2 - (\hat{x}_p^{i+1})^2}}{\hat{y}_p^{i+1} + j\hat{x}_p^{i+1}}\right),$$

$$c^i = \frac{\hat{x}_p^{i+1}\hat{y}_u^i - \hat{y}_p^{i+1}\hat{x}_u^i}{V_u^i\Delta t}$$

Figure 2.2: Trajectory Envelopes

A trajectory can be defined with three variables: velocity, heading, and the ratio of ECAV

3

range to phantom range (α). The resulting formulation is a single non-linear equation relating velocity to heading at a given point in space.

The pulse-to-pulse agility of the radar constrains the region of solutions, since the ECAV cannot go beyond the phantom in range ($0 < \alpha < 1$). The $\psi(V)$ equation yields two trajectory bounds when a minimum velocity is specified. These four bounds give rise to two envelopes of flyable trajectories (fig 2.2).

If the trajectories are to be continuous, the ECAV cannot arbitrarily switch between regions. This would require a large instantaneous change in heading. As trajectories evolve, the regions will expand and contract. It is possible for a region to collapse when the α and ψ bounds become collinear. When this occurs, the phantom track becomes infeasible. Note that the velocity equation becomes singular when

$$\hat{y}_p^{i+1} \sin \psi_u^i = \hat{x}_p^{i+1} \cos \psi_u^i$$

This represents the situation when the ECAV is flying parallel to the radar sightline.

If the regions expand such that the ψ bounds converge, it would be possible to switch from the ψ^+ to the ψ^- region. This only occurs in special cases where the ECAV motion allowed to be perpendicular to the radar sightline. This situation will be investigated further in the next section.

This set of ECAV constraints barely restricts the set of feasible phantom trajectories. Given a random phantom trajectory, it is usually possible to generate an ECAV trajectory. The only exceptions are the singular parallel case and when the lower envelope collapses. Since the phantom trajectory is itself a valid ECAV trajectory, choosing the upper envelope will cause the ECAV trajectory to asymptotically approach the phantom trajectory. Choosing the lower envelope will cause the ECAV to asymptotically approach the radar, until the V=Vmin bound is reached, collapsing the region.

2.2 Constant Velocity, Constrained Angle

For this set of constraints, it is convenient to change to polar coordinates. It is reasonable to assume that if the phantom track is given, that the angular velocity of the radar sightline can be determined. The ECAV velocity is constant, and is therefore given as well.

Given:

$V_u(t)$: Constant linear velocity of ECAV

$\dot{\theta}(t)$: Angular velocity of radar sightline
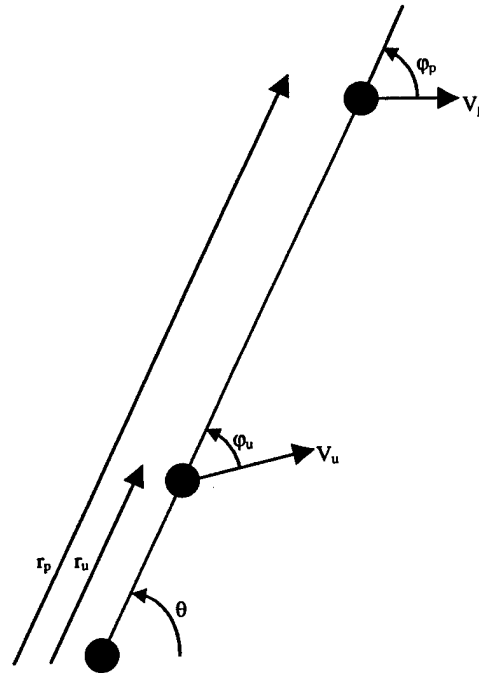
Find:

$r_u(t)$: Range of ECAV

Figure 2.3: Polar Coordinate System

Solution:

$$V_u^2 = V_{ur}^2 - V_{u\theta}^2$$

$$V_u \cos \varphi_u = \dot{r}_u$$

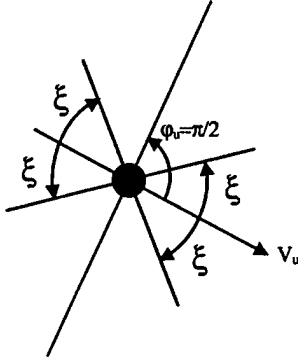$$V_u \sin \varphi_u = r_u \dot{\theta}$$

$$V_u^2 - \dot{r}_u^2 - r_u^2 \dot{\theta}^2 = 0 \quad : \quad \text{Nonlinear differential equation of motion}$$

4

Constraints:

$$\dot{r}_u^2 \geq 0 \rightarrow$$

$$r_u^2 \dot{\theta}^2 \leq V_u^2$$

$$r_u \leq \left|\frac{V_u}{\dot{\theta}}\right|$$

Figure 2.4: Bearing Angle Constraints

$$+\tfrac{\pi}{2} - \xi \leq \varphi_u \leq +\tfrac{\pi}{2} + \xi$$

$$-\tfrac{\pi}{2} - \xi \leq \varphi_u \leq -\tfrac{\pi}{2} + \xi,$$

$$0 < \xi < \tfrac{\pi}{2}$$

$$V_u \cos \varphi_u = \dot{r}_u \rightarrow$$

$$|\dot{r}_u| \leq |V_u| \cos \xi$$

$$V_u \sin \varphi_u = r_u \dot{\theta} \rightarrow$$

$$|r_u \dot{\theta}| \geq |V_u| \cos \xi$$

$$r_u \geq \left|\frac{V_u}{\dot{\theta}}\right| \cos \xi$$

The motion of the ECAV is governed by the solutions of the non-linear differential equation on r_u. Notice that the first constraint is imposed from the geometry of the problem itself. It implies that the range of the ECAV is bounded from above by the ratio of its velocity to its angular velocity about the radar station. Once the heading constraint is added, a lower bound is imposed on the range. This bound is equal to the preceding ratio times the cosine of the angle restriction. Note that this bound goes to zero as ξ goes to $\pi/2$, as expected.

When $\xi=0$, the ECAV is restricted to fly at a constant range, and the range rate ($\dot{r}$) is identically zero. This also agrees with the intuition provided from figure 2.4. In terms of the coordinates of section 2.1, the ψ bounds become the only valid trajectories when the ECAV velocity is kept constant. The phantom track becomes infeasible when the ψ bounds converge. This represents the situation when the ECAV is flying perpendicular to the radar sightline ($\xi=0$).
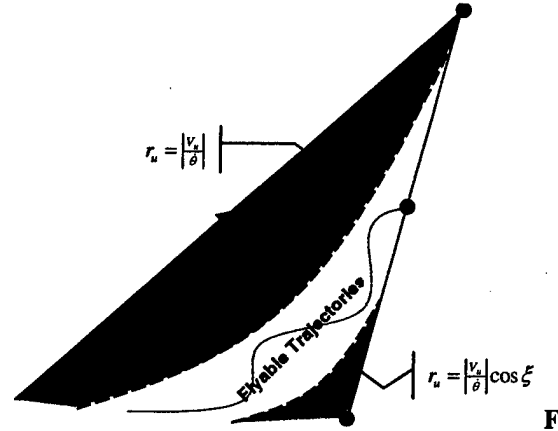
igure 2.5: Region of Flyable Trajectories

It is clear that this set of constraints imposes greater limits on the set of feasible phantom trajectories. This is generally going to be the case. The more restrictive the constraints, naturally, the more limited the set of feasible phantom trajectories will be.

3   Multiple ECAVs, Single Phantom

When multiple ECAVs are considered, the problem goes from being a simple geometry problem to a complex coordinated control problem. If the phantom track is determined *a priori* and the ECAV initial positions are known, it is also possible to determine the ECAV trajectories offline. This problem can be considered open loop from the systems perspective, but requires tight time synchronization. The major downside to this approach is its inherent lack of robustness. Unforeseen complications (wind, terrain, etc) will render this approach useless, unable to adapt to changing conditions.

A better approach would not require knowledge of initial conditions. The phantom trajectory could be determined online by a closed-loop cooperative team. Knowledge of an

5

"optimal" phantom trajectory could be imposed, but is not required.

Whether the control problem is considered decentralized depends the definition. Here, we consider decentralization to be a measure of the level of communication present in the system. A fully centralized system shares full state information for all team members. In a fully decentralized system, all team members operate without interaction. The amount of required communication is a function of the desired system performance. This does not *necessarily* imply any distribution in the computational load. Therefore, it makes sense to talk about a "leader" in the decentralized system. The leader may be virtual, where each team member does the same calculation based on the same shared information.

What makes this problem unique, and not redundant, is the strength of the required coordination. In this problem, if one ECAV fails, the team objective may not be obtainable. If one radar does not see what the other radars see, the track may be rejected. The fact that system performance does not degrade gracefully is an important aspect of the problem.

Generation of the phantom track is a negotiation problem. Each ECAV has physical constraints on where and how quickly it can move, further limited by operational constraints on speed and heading. Based on this knowledge, an ECAV generates a cost-to-go function that represents the cost to move to a particular location. The function changes with time, depending on the local state. The leader must aggregate the individual cost functions to form a coherent minimum-cost path.

The cost-to-go function of an ECAV represents the current and future cost of moving to a particular location. The effort to move to a particular location and the time-horizon impact of such a move must be incorporated. The effort cost is a function of the current heading and speed. An ECAV is physically bounded by turning rate and acceleration constraints. There will also be regions of heading and speed that are operationally favorable. Antenna directionality, fuel consumption, and radar cross-section pose operational limitations. When n-ECAVs are participating in deceiving n-radars, in an n-out-of-m radar network configuration, the team is meeting its objective. When one ECAV falls out of the team, the phantom track loses its coherency. There are finite regions of possible trajectories, so the

cost functions must attempt to "steer" the ECAV toward more favorable regions to maximize the time-horizon.

The radar deception system can be treated as a hierarchical decomposition of team goals into individual cost functions. A leader aggregates individual costs to determine an optimal team goal (phantom trajectory). It is up to the individual ECAVs to execute their trajectories to accomplish the goal. The determination of the team goal is an independent problem. It can be considered by assuming that the individual cost functions are known.

Aggregation techniques can be sub-optimal (heuristic) or optimal. To take the heuristic approach, the leader considers several phantom trajectory alternatives. The ECAVs report the cost of each alternative to the leader. If there is a preconceived notion of a "best phantom path", this is used to apply weights the ECAV costs. This notion may be an operational goal of drawing the radars away from a particular region or to maintain a constant phantom heading or speed. If no such restriction is imposed, a minimum-sum approach is used to pick the best phantom path. This heuristic technique is called optimalization.

The alternative approach is to find the optimal phantom path directly through optimization. One popular technique is Model Predictive Control (MPC), where the phantom is the control object. The individual ECAV cost functions and any "best phantom path" notions are combined into a single phantom cost function. Physical restrictions on the phantom can be imposed as constraints. The phantom track is determined by solving this constrained optimization problem at each step.

The optimality of the heuristic approach can be improved by considering more alternatives at the expense of speed. The speed of the MPC approach can be improved by limiting the number of iterations at the expense of optimality. The tradeoff between optimality and speed is the same, and either approach is feasible.

From a communications standpoint, the heuristic approach is less demanding than the MPC approach. Only the scalar cost alternatives need to be passed around. In the optimal problem, functions of several variables need to be passed around at each step. The communication delays need to be minimized to maintain the stability of the system.

6

The output of the path planner can be represented as a set of waypoints, equally spaced in time. The phantom path planning problem could be thought of as a set of successive cooperative rendezvous problems, where the rendezvous points are variable, but the times are not. Along those lines, one strategy for minimizing communication is to negotiate the entire phantom path at the beginning. Once the path has been agreed upon, it will be executed and only reconsidered if complications arise (wind, terrain, etc). The ECAVs could be implemented as three-state machines. Initially, all ECAVs start in the autonomous flight state until the deception is initiated. At this time, the entire phantom trajectory is negotiated and shared among team members. Once the plan is complete, the individual ECAVs execute the plan, unless a re-plan becomes necessary or until the deception is complete. If a suitable phantom track cannot be negotiated, the vehicles return to autonomous flight and reposition themselves to try again.
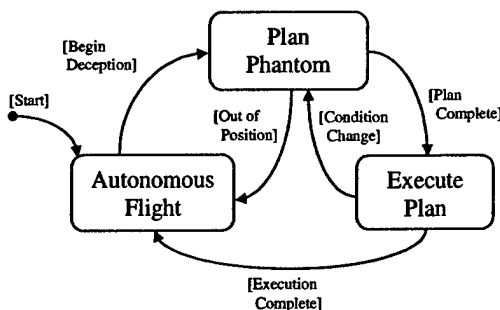

Figure 3.1: State Flow Diagram

It is assumed that the individual ECAVs can generate trajectories to hit the waypoints on time. If this is not the case, the phantom plan is flawed and must be renegotiated. The specifics of ECAV trajectory planning (Voronoi diagrams, etc) have a thorough treatment in the literature, and are not considered here.

4 Multiple ECAVs, Multiple Phantoms

Once the multiple ECAV, single phantom case has been considered, it is natural to try to extend it to generate multiple phantom tracks. This is not possible in general, however. Under special circumstances it may be possible to generate secondary tracks, but they will not last as long as the primary track, and they will not be independent.

With a single ECAV and single radar, it is possible to generate a string of collinear returns by varying the range delay. Once a second radar and ECAV are added to the scenario, the radar sight lines will intersect at exactly one point. Once a third radar and ECAV are added, the radars will intersect at most at one point.

In special geometric configurations where only 2-out-of-n radars need to concur, it could be possible to generate many phantom tracks with only one ECAV. For example, in the following configuration (fig 4.1), the ECAV (green) can send returns to three pairs of radars (red) at once, effectively generating 3 confirmed phantoms (black) independently. Note that the motions of the phantoms are necessarily coupled. The limitations of this scenario are obvious. If the radar network requires 3-out-of-n radars or if the geometric shape doesn't hold, the phantoms vanish.
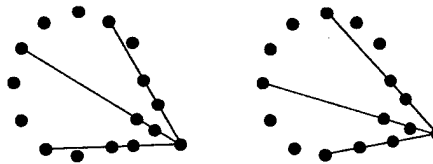

Figure 4.1: Single ECAV, multiple radars, and multiple phantoms

This is just an example of what could be done. Most geometric scenarios like this break down quickly, and are almost definitely impossible in a 3-out-of-n or greater radar network.

Another way to generate multiple phantoms with n-ECAVs and n-radars in an n-out-of-m network is through side-lobe manipulation.

A radar antenna emits energy in all directions (figure 4.2) and receives energy in all directions.
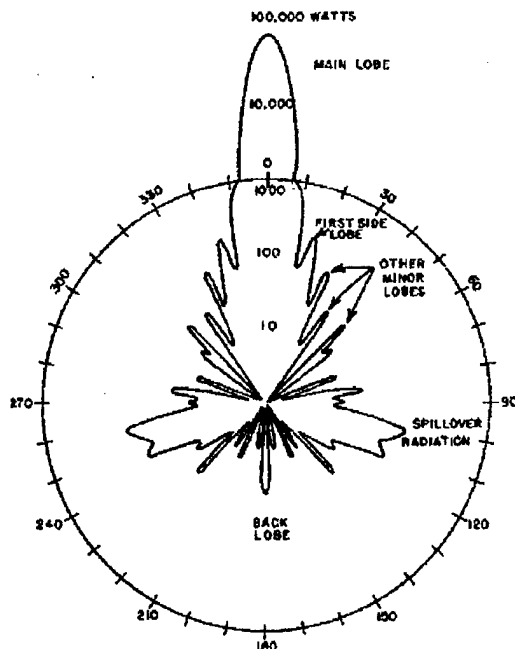
Figure 4.2: Typical Radar Radiation Pattern

In some cases, it may be possible to echo a side-lobe pulse, fooling a radar into believing something is in front, when it is actually aligned with a side-lobe. Figure 4.3 demonstrates this principle. In general, this is also not sustainable. The radars employ sophisticated filters to eliminate side-lobe noise. While it may be possible to overwhelm these filters, it is unlikely. Unless you are injecting energy directly along one of the primary side-lobes, there will be little chance of creating a strong enough return.
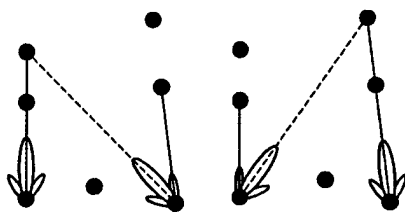
Figure 4.3: Two radars, Two ECAVs, Two Phantoms

5 Additional Radar Considerations

An attempt has been made to abstract the findings of this paper from the specifications of the radar being employed. The purpose of this section is to investigate a few important considerations that are specific to the radar specifications.

5.1 Uncertainty

Before any inference on the feasibility of this radar deception scenario can be made, a thorough study of the uncertainty must be made. As is often the case, the uncertainty is a dominant problem.

There are many potential sources of uncertainty in this problem. A certain amount of uncertainty can be tolerated in the positioning of the ECAVs. The radars have a beam width of a few degrees, so at a great range, there will likely be sufficient room to operate. If the phantom point jumps around a little from pulse to pulse, this is also not a big problem. If the phantom were an actual aircraft, the radar echoes would fluctuate as the aircraft pitches and rolls.

Of greater concern is uncertainty in the position of the radars themselves. Many successive errors have the potential of defeating the coordination. It may be possible to triangulate the radar positions based on incoming pulse amplitudes. This data could be filtered to obtain an improving estimate on radar positions. This estimation problem could prove to be just as important and challenging as the ECAV positioning.

Another area of concern is unforeseen delays in communication. There must be some type of information synchronization protocol. If the phantom trajectory is agreed upon before it is executed, on-line communication will be at a minimum and delays shouldn't pose a major problem. The information synchronization during the planning phase is of greater concern.

Every scenario discussed in this study assumes tight clock synchronization. If the clocks do not coincide on the nanosecond scale, the echoes will not have the precise range delay that is required to make the phantom track converge. Signal processing delay is another potential problem. Even if the clocks were dead-on, a slight unforeseen delay in processing would extend the range delay, destroying the synchronization. These timing uncertainties could also prove to be one of the most difficult challenges.

5.2 Radar PRF and Scan Modes

The pulse repetition frequency (PRF) of ground radar determines its sensing capabilities. Low-PRF radar has large Doppler ambiguities,

8

poor main-lobe noise rejection, but good side-lobe rejection. High-PRF radar has large range ambiguity and the opposite noise-rejection characteristics. The primary source of main-lobe clutter in airborne radar is from ground return. In upward looking ground radar, this is not a factor.

For the ECAV scenario, three primary modes of deception are possible: low-PRF main-lobe range deception, high-PRF main-lobe Doppler deception, and high-PRF side-lobe Doppler deception. In a practical scenario, the radars would switch between high and low PRF modes. To effectively generate a phantom point, it is necessary to provide both range delay and Doppler deception at all times. If multiple tracks are being generated through the side-lobes, the additional tracks will only be detected when the radars are in a high-PRF mode. This may pose a problem with track credibility.

In addition to the PRF, there are three scan modes in which the ground radar can operate: search, track, and track-while-scan (TWS). In search mode, the radar is in early detection mode, performing a slow and wide multi-bar scan. When operating in high-PRF mode, this is called velocity search (VS), because it detects objects that are closing or opening at a significant speed. In low-PRF mode, this is called range while search (RWS), because it can detect the range of multiple objects at various headings, with low accuracy. At the other end of the spectrum is single track (ST) mode. In this mode, the radar locks on an object and continually monitors it, providing a highly accurate measure of the object position and velocity, but unable to detect new objects. In radars with electronically steered antennas (ESA), it is possible to simultaneously track multiple objects with little degradation in accuracy. A compromise of these two modes is TWS mode. This performs a multi-bar scan to periodically check the position of multiple objects while searching for new objects. This mode can also track multiple objects, but with lesser accuracy than ST. The discreet nature of the radar scan pattern justifies our choice of specifying discreet waypoints uniformly spaced in time.

It can be assumed that the radars are in either ST or TWS mode. If the radars are in a radar network, they will require corroboration. The only significant difference is that in TWS mode, it may be advantageous for the ECAV to provide additional false returns. This will cause the radars to spend time investigating new objects. Even though these phantom points will not be corroborated and thus discarded, performance will be degraded. This will affect the ability of the network to accurately sense the phantom track, which will in turn make it easier to generate.

It is assumed that the radar is operating at a low duty-cycle. This is necessary because of the limited processing capabilities of the ECAV. This is especially critical in the case where the ECAV is attempting to deceive multiple radars at once through the side-lobes.

6 Conclusions

A radar deception scenario that employs a cooperative multi-agent team has been considered. It appears that from the analysis to date that the scenario is theoretically feasible. Given a set of constraints, a first step is to determine the regions of operability for the ECAV. If the results are satisfactory, cost functions must be developed to relate ECAV trajectories to ECAV effort and the time-horizon. Similarly, preferred phantom trajectories should be considered and used to aggregate the ECAV cost functions. It still remains to be seen whether the system is practically feasible due to the complications of uncertainty. Generation of multiple phantom tracks is only realistic in very specific situations. Simulations should be performed to confirm the viability of the distributed cooperative control scheme. A sensitivity analysis should be performed to study the effect of uncertainties on the convergence of the system. This is left as future work.

References

[1] T.W. McLain, P.R. Chandler, S. Rasmussen, M. Pachter, Cooperative Control of UAV Rendezvous, Proc. of the American Control Conference (2001), pp. 2309-2314.

[2] R.W. Beard, V. Stepanyan, Synchronization of Information ion Distributed Multiple Vehicle Coordinated Control, IEEE Conference on Decision and Control, 2003.

[3] G.W. Stimson, Introduction to Airborne Radar, Raleigh, NC: SciTech Publishing, 1998.

[4] S.A. Vakin, L.N. Shustov, R.H. Dunwell, Fundamentals of Electronic Warfare, Norwood, MA: Artech, 2001.

Appendix A: Matlab Code (easim.m)

```
clear all
close all

dt = .2;   %Step Size
n = 500; %Sim Length
beamwidth = pi/3;

% Initial Conditions
axp = 0;
ayp = 0;
vxp = 100*sin(pi/4); % m/s
vyp = 100*cos(pi/4);
alpha = [0.4];
xp = 0; % m
yp = 1000; % m
xr = [3000 8000]; % m
yr = [1000 1000]; % m
xu = xr-(xr-xp).*alpha; % m
yu = yr-(yr-yp).*alpha; % m
s = 1; %direction

rp = sqrt((xp-xr(2))^2+(yp-yr(2))^2);
th = atan2(xp-xr(2),yp-yr(2));

vmin = 100; % m/s
vpmin = vmin/0.5; %m/s

for i=1:n-1
    % Generate Random Phantom Trajectory
    axp(i+1) = 100*(0.5-0.5); %5Gs
    ayp(i+1) = 100*(0.5-0.5); %5Gs
    vxp(i+1) = vxp(i)+axp(i+1)*dt;
    vyp(i+1) = vyp(i)+ayp(i+1)*dt;

    v(i) = sqrt(vxp(i+1)^2+vyp(i+1)^2);
    if (v(i) < vpmin)
            vxp(i+1)=vpmin/v(i)*vxp(i+1); %Stall Speed
            vyp(i+1)=vpmin/v(i)*vyp(i+1); %Stall Speed
    end
    xp(i+1) = xp(i)+vxp(i+1)*dt;
    yp(i+1) = yp(i)+vyp(i+1)*dt;

    % Generate Circular Phantom Trajectory
%    xp(i+1) = xr(2) + rp*sin(vpmin*dt/rp*(s*(i-1))+th(1,1));
%    yp(i+1) = yr(2) + rp*cos(vpmin*dt/rp*(s*(i-1))+th(1,1));

    clf
    plot(xp(1:i+1),yp(1:i+1)); %Plot phantom trajs
    hold on;
    plot(xp(i+1),yp(i+1),'*');

    % Generate ECAV Trajectories
    for j=1:size(xr,1)

        xpij = xp(i+1)-xr(j); %Change Basis
        ypij = yp(i+1)-yr(j);
        xuij = xu(j,i)-xr(j);
        yuij = yu(j,i)-yr(j);

        plot(xu(j,1:i),yu(j,1:i),'g'); % Plot ECAV trajs
        plot(xu(j,i),yu(j,i),'go');
        plot([xr(j) xp(i+1)],[yr(j) yp(i+1)],'r')
        plot(xr(j),yr(j),'ro');
        r(j,i) = sqrt(xuij^2+yuij^2);
        th(j,i) = atan2(xpij,ypij);

        if (i>1)
```

```
                  rd(j,i) = (r(j,i)-r_old)/dt;
                  thd(j,i) = (th(j,i)-th_old)/dt;
                  ax=axis;

plot(s*(vmin./thd(2:end).*sin(th(2:end)))+xr(j),s*(vmin./thd(2:end).*cos(th(2:end)))+yr(j
),'k')
                  plot(s*(vmin*sin(pi/2-
beamwidth)./thd(2:end).*sin(th(2:end)))+xr(j),s*(vmin*sin(pi/2-
beamwidth)./thd(2:end).*cos(th(2:end)))+yr(j),'k')
                  text(diff(ax(1:2))*.1+ax(1),diff(ax(3:4))*.95+ax(3), ['rd = '
num2str(rd(j,i))])
                  text(diff(ax(1:2))*.1+ax(1),diff(ax(3:4))*.90+ax(3),['r*thd = '
num2str(r(j,i)*thd(j,i))])
                  text(diff(ax(1:2))*.1+ax(1),diff(ax(3:4))*.85+ax(3),['radar angle = '
[num2str(acos(rd(j,i)/vmin)*180/pi-90) '°']])
                  if abs(r(j,i)*thd(j,i)/vmin)<sin(pi/2-beamwidth)
                      disp('Lost Sight of Radar');
                      return;
                  end
              end
          r_old=r(j,i);
          th_old=th(j,i);
          M(i) = getframe;
          c=-(xpij*yuij-ypij*xuij)/(vmin*dt);
          bounds=[-1i*log((c-sqrt(c^2-ypij^2-xpij^2))/(xpij+1i*ypij))...
                  -1i*log((c+sqrt(c^2-ypij^2-xpij^2))/(xpij+1i*ypij))];

          if (imag(bounds)<.001)
          else
              disp('No valid trajectories');
              return;
          end

          psiu(j,i) = real(bounds(2));

          vu(j,i) = (xpij*yuij-ypij*xuij)/((ypij*sin(psiu(j,i))-xpij*cos(psiu(j,i)))*dt);

          xu(j,i+1) = xu(j,i)+vu(j,i)*sin(psiu(j,i))*dt;
          yu(j,i+1) = yu(j,i)+vu(j,i)*cos(psiu(j,i))*dt;
          alpha(j,i+1) = (yu(j,i+1)-yr(j))/ypij;

          if (alpha(j,i+1) < 0) | (alpha(j,i+1) > 1)
              disp('Error: No solution');
              return;
          end


      end

end


figure
subplot(2,1,1)
plot(alpha')
subplot(2,1,2)
plot(vu')
```